tvst

DOI: 10.1167/tvst.5.6.7

Article

ROCK Inhibition Promotes Attachment, Proliferation, and Wound Closure in Human Embryonic Stem Cell–Derived Retinal Pigmented Epithelium

Roxanne H. Croze, William J. Thi, and Dennis O. Clegg

Center for Stem Cell Biology and Engineering, Neuroscience Research Institute, Department of Molecular, Cellular & Developmental Biology, University of California, Santa Barbara, CA, USA

Correspondence: Dennis O. Clegg, University of California, Santa Barbara, Neuroresearch Institute, Building 571, Room 6131, Santa Barbara, CA 93106, USA. e-mail: dennis.clegg@lifesci.ucsb.edu

Received: 4 June 2016
Accepted: 10 October 2016
Published: 22 November 2016

Keywords: age related macular degeneration; retinal pigment epithelium; ROCK inhibition

Citation: Croze RH, Thi WJ, Clegg DO. ROCK inhibition promotes attachment, proliferation, and wound closure in human embryonic stem cell–derived retinal pigmented epithelium. Trans Vis Sci Tech. 2016; 5(6):7, doi:10.1167/tvst.5.6.7

Purpose: Nonexudative (dry) age-related macular degeneration (AMD), a leading cause of blindness in the elderly, is associated with the loss of retinal pigmented epithelium (RPE) cells and the development of geographic atrophy, which are areas devoid of RPE cells and photoreceptors. One possible treatment option would be to stimulate RPE attachment and proliferation to replace dying/dysfunctional RPE and bring about wound repair. Clinical trials are underway testing injections of RPE cells derived from pluripotent stem cells to determine their safety and efficacy in treating AMD. However, the factors regulating RPE responses to AMD-associated lesions are not well understood. Here, we use cell culture to investigate the role of RhoA coiled coil kinases (ROCKs) in human embryonic stem cell–derived RPE (hESC-RPE) attachment, proliferation, and wound closure.

Methods: H9 hESC were spontaneously differentiated into RPE cells. hESC-RPE cells were treated with a pan ROCK1/2 or a ROCK2 only inhibitor; attachment, and proliferation and cell size within an in vitro scratch assay were examined.

Results: Pharmacological inhibition of ROCKs promoted hESC-RPE attachment and proliferation, and increased the rate of closure of in vitro wounds. ROCK inhibition decreased phosphorylation of cofilin and myosin light chain, suggesting that regulation of the cytoskeleton underlies the mechanism of action of ROCK inhibition.

Conclusions: ROCK inhibition promotes attachment, proliferation, and wound closure in H9 hESC-RPE cells. ROCK isoforms may have different roles in wound healing.

Translational Relevance: Modulation of the ROCK-cytoskeletal axis has potential in stimulating wound repair in transplanted RPE cells and attachment in cellular therapies.

Introduction

Age-related macular degeneration (AMD) is a progressive disease that is the leading cause of blindness in the aged population of the developed world.[1] While the mechanisms underlying AMD are still under investigation, most evidence suggests that death or dysfunction of the retinal pigmented epithelium (RPE) is responsible for onset of the disease. The RPE cells are critical for maintaining the function and viability of the photoreceptors, the main light sensing neuron. Therefore, when the RPE cells degenerate, the photoreceptors in turn begin to die and vision is lost.[2,3]

There are two forms of the disease, wet or exudative, and dry or atrophic AMD. Wet AMD is characterized by neovascularization, which disrupts the RPE monolayer. This form, although rapidly progressive, can be treated with intraocular injections of anti–vascular epithelial growth factor (VEGF) antibodies to suppress the overactive blood vessel formation.[1] The dry form, affecting 80% to 90% of patients diagnosed with AMD, can only be treated with a vitamin cocktail and antioxidant supplements, which merely slows disease progression in 25% of patients.[4,5] Geographic atrophy (GA), areas devoid of RPE cells and photoreceptors, often occurs in late stage AMD patients, leading to large deficits in the central visual field. Unfortunately, RPE have limited proliferative abilities to fill in areas affected by GA prior to photoreceptor death.[6,7]

RPE cell therapy has potential for treating AMD and other ocular diseases that affect RPE cells[8,9]; and is currently in clinical trials for both AMD and Stargardt's disease.[10,11] A number of groups are investigating RPE derived from induced pluripotent stem cells (iPSC), human embryonic stem cells (hESC), and adult RPE, introduced as either a bolus injection or as a monolayer on a scaffold.[12] A Phase 1/2A clinical trial has been initiated using H9 hESC-RPE on a parylene scaffold, which is the first in human use of the widely studied H9 hESC line. An additional strategy would be to stimulate repair mechanisms in the transplanted cells to bring about migration to and repopulation of areas where cells are lost, such as GA. In this study, we investigate potential wound healing strategies in H9 hESC-RPE cells.

Epithelial wound healing is initiated by proliferation of epithelial cells in response to wound-related cytokines.[13] This is followed by a remodeling and maturation phase where activated myofibroblasts, which result from an epithelial to mesenchymal transition (EMT), stimulate contraction of the epithelium, migration, and regeneration.[13] In chronic wounds, excessive inflammatory cells lead to the failure to restore a normal epithelium, resulting in fibrotic scarring.[14,15]

Dynamic regulation of the cytoskeleton is important in cell attachment, migration, and contraction events that are critical to wound healing.[16] GTPase activated Rho-associated coiled-coil kinases (ROCKs) are key regulators of cytoskeletal rearrangement through the regulation Lin11, Isl-1, Mec-3 (LIM) kinase/cofilin activity.[17] LIM domain proteins are also known to regulate transforming growth factor-β (TGF-β) signaling and affect EMT in wound healing.[18] Two human isoforms, ROCK1 and ROCK2, have been shown to play distinct roles in cytoskeletal regulation.[19–23] ROCKs have been investigated in a variety of diseases,[24] and ROCK inhibition, using synthetic inhibitors, is being examined as a treatment option for pulmonary hypertension,[25] cancer,[26] glaucoma,[27] and certain neurological diseases.[28,29] In the retina, intravitreal injections of Y-27632, a synthetic pan ROCK inhibitor, were shown to protect photoreceptors from apoptosis and support retinal structure and function in the Royal College of Surgeons rat, a model of retinal dystrophy; however, RPE cells were not examined.[30]

ROCK inhibition also boosts proliferation rates of hESC-RPE and allows hESC-RPE and iPSC-RPE cells to be continually passaged in culture for over 10 passages prior to senescence and appears to inhibit TGF-β signaling, the main pathway driving EMT.[31] Based on the known effects of ROCK inhibition on proliferation and the cytoskeleton, we hypothesized that ROCK inhibition would affect wound healing and substrate attachment in hESC-RPE. We show that pharmacological inhibition of ROCK activity stimulates attachment and proliferation of hESC-RPE, and augments wound closure in vitro. ROCK inhibition has the potential to stimulate proliferation of endogenous or transplanted RPE cells to fill in areas affected by AMD or GA.

Methods

Derivation and Maintenance of hESC-RPE Cells

H9 hESC were acquired from WiCell (Madison, WI) and were cultured on Matrigel in mTESR1. Medium was changed every other day and cells were kept at 37°C in 5% CO_2 in normoxic conditions. H9 hESC-RPE cells were the focus of these experiments because they are currently in clinical trials.

H9 hESC were overgrown for 8 to 14 days, followed by the removal of basic fibroblastic growth factor and a medium change to XVIVO-10 (Lonza, Basel, Switzerland). Cells were cultured for 90 to 120 days with a medium change every 2 to 3 days. After 90 to 120 days, the nonpigmented cell patches were manually excised and washed away using phosphate buffered saline (PBS; Life Technologies, Carlsbad, CA). Pigmented patches were lifted from the plate following a 5-minute incubation at 37°C with TrypLE Express (Life Technologies). Cells were then diluted in XVIVO-10, spun for 5 minutes at 1000 rpm, and plated at 1.0×10^5 cells/cm^2 on Matrigel-coated 6-well plates (BD Biosciences, San Jose, CA). Every 30 days, these enriched RPE were again enzymatically passaged using TrypLE Express. Medium was changed every 2 to 3 days. Cells used in experiments were between passages 1 and 4. At least three individual enrichments derived from distinct H9 cultures were used for all analyses.

Quantification of Cell Attachment

hESC-RPE cells were passaged as described above, and seeded at 1.0×10^5 cells/cm^2 on Matrigel-coated eight-chambered slides in XVIVO-10. At the time of plating, cells were treated with 10-μM Y-27632 (pan ROCK inhibitor), 10-μM ROCKIV (ROCK 2 isoform only inhibitor), or an equal volume of water as a

control (Tocris, Minneapolis, MN). Cells were allowed to attach for 1, 2, 4, 6, and 24 hours. At each time-point, attached living cells were stained with Calcein AM according to manufacturer's instructions using a LIVE/DEAD Cytotoxicity Kit (Life Technologies). Cells were then fixed for 1 hour at 25°C in 4% paraformaldehyde (PFA) in PBS. Attached cells were visualized through fluorescent microscopy using an Olympus BX51 microscope at a ×10 objective (Olympus, San Jose, CA). The same three areas of each chamber were imaged for each condition within each time-point. Fluorescent quantification was analyzed by integrated pixel density with a rolling ball radius of 50 and background subtraction using Fiji software.[32] Each treatment was represented as the percent of the sum total fluorescence for the corresponding time point to eliminate the variability of dye intensity between experiments, but preserving the change between treatments.

Quantification of Cell Spreading

hESC-RPE cells were plated and treated as described for the quantification of attachment. Cells were allowed to attach for 1, 2, and 4 hours. Cells were then fixed in 4% PFA in 0.1M cacodylate buffer for 15 minutes at 4°C. Cells were blocked and permeabilized in 5% bovine serum albumin (BSA) plus 0.2% Triton X-100 for 1 hour at 4°C. Phalloidin conjugated to Tetramethylrhodamine (TRITC; 220 μM; Life Technologies) was added to the cells in PBS for 45 minutes at 4°C to label F-actin. Hoescht dye (2 μg/mL; Life Technologies) was then added and incubated at 25°C for 5 minutes to stain cellular DNA. Cell area was determined through visualization of FITC staining by fluorescent microscopy at 60× on a BX51 Olympus microscope and analyzed using the Fiji software polygonal tool, outlining the cells; 20 cells per image in internal triplicate, with at least three independent experiments per time-point.

Western Blotting

hESC-RPE cells were passaged onto Matrigel-coated T-25 flasks and treated as in the quantification of attachment. Two hours after plating, cells were washed two times with Hanks Balanced Salt Solution for 10 minutes each (HBSS; Life Technologies). Cells were lysed in a RIPA buffer with protease and phosphatase inhibitor tablets (Roche, Basal, Switzerland). Cells were then incubated on ice for 15 minutes and spun at 13,000 rpm for 5 minutes. Lysates were stored at −80°C until use. A bicinchoninic acid assay (BCA; Life Technologies) was performed to determine protein concentration. Fifty micrograms of protein was loaded and run on a 12.5% acrylamide gel, followed by a transfer to a nitrocellulose membrane. The membrane was blocked for 1 hour at 25°C in 5% BSA in Tris-Buffered Saline plus Tween-20 solution (TBST). Myosin Light Chain 2 (MLC 2; 1:1000; Cell Signaling Technology, Danvers, MA), MLC phoshpo-S20 (1:1000; Abcam, Cambridge, UK), Cofilin (1:1000; Cell Signaling Technology), Cofilin phospho-S3 (1:1000; Cell Signaling Technology), and Beta-actin (1:1000; Cell Signaling Technology) primary antibodies were added in block and incubated overnight at 4°C. Primary antibodies were washed three times in TBST and then LI-COR secondary antibodies (1:2000; LI-COR, Lincoln, NE) were added in block for 1 hour at 25°C and fluorescence was detected on a LI-COR imager after three TBST washes.

All images were taken using the LI-COR imager with the same settings and exposures, and Fiji processing techniques. The integrated pixel density of each band was quantified in Fiji using a background subtraction with a rolling ball radius of 50. Phosphorylation quantification was divided by β-actin quantification to account for differences in protein loading.

Scratch Assay

hESC-RPE cells were grown for 30 days in XVIVO-10 in a 12-well plate. Using a P200 pipet tip, a scratch was created down the center of the well from the top to the bottom on day 30. Cells were washed three times with PBS. Ten micromolar of Y-27632 (pan ROCK inhibitor), 10 μM of ROCKIV (ROCK2 inhibitor), or an equal volume of water as a control was added to cells in fresh XVIVO-10 for 14 days post scratch. Immediately following the scratch, cells were imaged along the wound and will be identified as day 0, three images per well. The cells were also imaged 3, 7, and 30 days post scratch. Quantification of the area of the wound closure was determined using the Fiji polygonal tool to outline the area devoid of cells at day 0, and subsequently at day 3, 7, and 30. The areas were then subtracted from the day 0 area and divided by the day 0 area, then made into a percent to represent percent wound closure.

Immunoctyochemistry (ICC)

On day 5 and 30 after scratch, cells were fixed with 4% PFA in 0.1M cacodylate buffer for 15 minutes at

4°C. Cells were then blocked with 5% BSA plus 0.2% Triton X-100 for 1 hour at 4°C. Primary antibody for MKI67, marker of proliferation KI67, was diluted in block (1:1000; Abcam) and incubated at 4°C overnight. The next day, the cells were washed three times with PBS. The corresponding 488 Alexa Fluor secondary antibody (1:300; Life Technologies) and Phalloidin conjugated to TRITC (220 μM; Life Technologies) were added to the cells in PBS for 45 minutes at 4°C. Hoescht dye (2 μg/mL; Life Technologies) was then added and incubated at 25°C for 5 minutes to stain cellular DNA. Cells were washed three times with PBS and mounted using Prolong Gold Anti-fade reagent (Life Technologies). Fluorescent microscopy was used to analyze expression patterns at 20× objective on an Olympus IX71 Microscope. Fiji and Microsoft Excel software (Microsoft Corporation, Redmond, WA) were used to quantify the integrated pixel density of MKi67 fluorescence within scratched region. Cell area was determined by outlining cells within the scratched region using the polygonal tool within Fiji and quantifying the area. Twenty cells were analyzed per image using internal triplicates and three separate experiments using independent enrichments.

Statistical Analysis

One-way analysis of the variance and Tukey's post hoc statistical tests were run within each time-point to compare control, Y-27632, and ROCKIV treatments, using a value of P less than 0.05 to claim significance.

Results

ROCK Inhibition Promotes Attachment Through an Increase in Cell Spreading and Cofilin Activation

ROCK activates LIMK through phosphorylation, leading to cofilin phosphorylation and inactivation, resulting in actin stabilization.[17] ROCK is also known to regulate stress fiber formation through the phosphorylation of MLC.[33] Therefore, inhibition of ROCK would be predicted to dephosphorylate cofilin and MLC and lead to actin depolymerization. Such reorganization of the cytoskeleton could affect cell attachment, but this has not been investigated in RPE cells.

Adhesion of hESC-RPE cells to matrigel was examined in the presence of ROCK inhibitors (Fig. 1). PanROCK (Y-27632) and ROCK 2 inhibition (ROCKIV) significantly promoted attachment of cells as early as 1 hour after plating, and this effect was maintained at all time-points examined, with the exception of Y-27632 compared with control at 2 hours; however, these data followed the trend (Fig. 1B). Both inhibitors resulted in approximately a 4-fold increase in adherent cells.

To examine cytoskeletal organization and cell spreading during cell attachment, F-actin distribution was analyzed by staining with phalloidin-TRITC (Fig. 2A). At 1, 2, and 4 hours after plating cells were fixed, permeabilized, and probed to visualize F-actin. PanROCK inhibition significantly increased cell spreading 1 hour after plating when compared with control cells, as determined by the calculation of cell area outlined from F-actin expression (Fig. 2B). This effect persisted at 2 and 4 hours after plating. ROCK2-specific inhibition further increased cell spreading at all time-points examined compared with panROCK inhibition, indicating a dominate role of ROCK2 inhibition in cell spreading.

Next, we investigated the phosphorylation states of cofilin and MLC proteins 2 hours after plating. Inhibition of ROCK in hESC-RPE cells decreased the amount of phosphorylated cofilin (Fig. 3A) and MLC (Fig. 3C). Densitometry of phosphorylated cofilin and MLC protein bands was determined and quantified in Figures 3B and 3D, respectively. We found that the ROCK2-specific inhibitor decreased phosphorylation of both proteins by approximately half. Curiously, the panROCK inhibitor decreased levels of phosphorylation but not significantly, suggesting a difference of effect between the two isoforms. No significant difference was seen in total cofilin or total MLC protein levels between treatments (Figs. 3A, 3C).

ROCK Inhibition Promotes Wound Closure In Vitro

hESC-RPE cells were grown for 30 days and then scratched to mimic a wound and monitored for an additional 30 days. PanROCK inhibition significantly enhanced wound closure compared with control by day 3 (Fig. 4A). ROCK2 inhibition showed significant wound closure by day 3 as well; however, the cell morphology within the scratched area was large and mesenchymal-like, not typical of the RPE (Supplementary Fig. 1). PanROCK inhibition and ROCK2 inhibition exhibited a higher percent of wound closure at every time-point examined (Fig. 4B). By day 30, the panROCK-inhibited cells com-

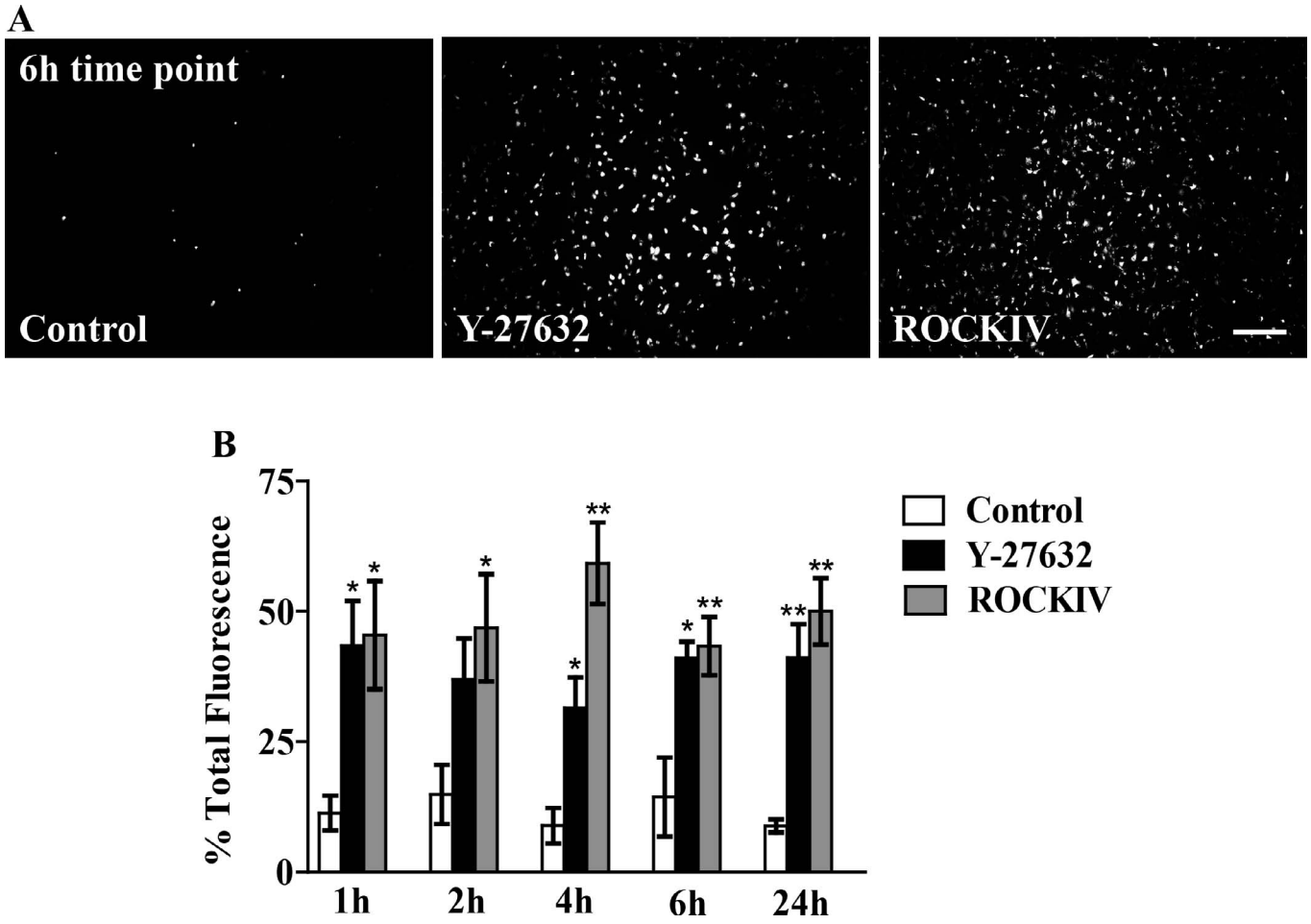

Figure 1. ROCK inhibition increases cell attachment. (A) Cells were stained with a Calcein AM dye to detect adherent and living cells. Fluorescent images at the 6-hour time-point are shown for all three treatments. *Scale bar*, 200 μm. (B) Quantification of adherent cells at time-points indicated. *$P \leq 0.05$, **$P \leq 0.01$ compared with control at that time-point. *Error bars* represent ± SEM ($n \geq 6$). Y-27632, panROCK inhibitor (10 μM); ROCKIV, ROCK2 inhibitor (10 μM).

pletely closed the wound, while the control cells failed to regain a confluent monolayer in the scratched space. ROCK2-inhibited cells showed significantly more wound closure than control at day 30; however, the larger cells seen in the earlier time-points persisted (Supplementary Fig. 1).

Interestingly, cells regained their epithelial morphology by day 7 following panROCK inhibition. Although control cells failed in fill in the entire scratched area by day 30, the cells present in the wounded space have mainly recovered their epithelial morphology. In contrast, ROCK2 inhibited cells, although fast to close the wounded area, still had flatter and more mesenchymal-like cells compared with control and Y-27632-treated cells at day 30 (Fig. 4).

PanROCK Inhibition Promotes Proliferation at Wound Site

A general concept of epithelium wound healing is that cells undergo an EMT that allows them to migrate into the area devoid of cells and form scar tissue or revert back through mesenchymal-to-epithelial transition (MET), closing the wound.[14] We hypothesized in our wound healing system, based on the known effects of ROCK inhibition on proliferation, that the increase in wound closure was in part due to an increase in proliferation.[31] Five days after the scratch, cells were subjected to immunocytochemistry and probed with an antibody against MKI67, a proliferation marker, and phalloidin, an F-actin probe, to analyze cytoskeletal arrangements (Fig. 5A). There was a significant increase in MKI67

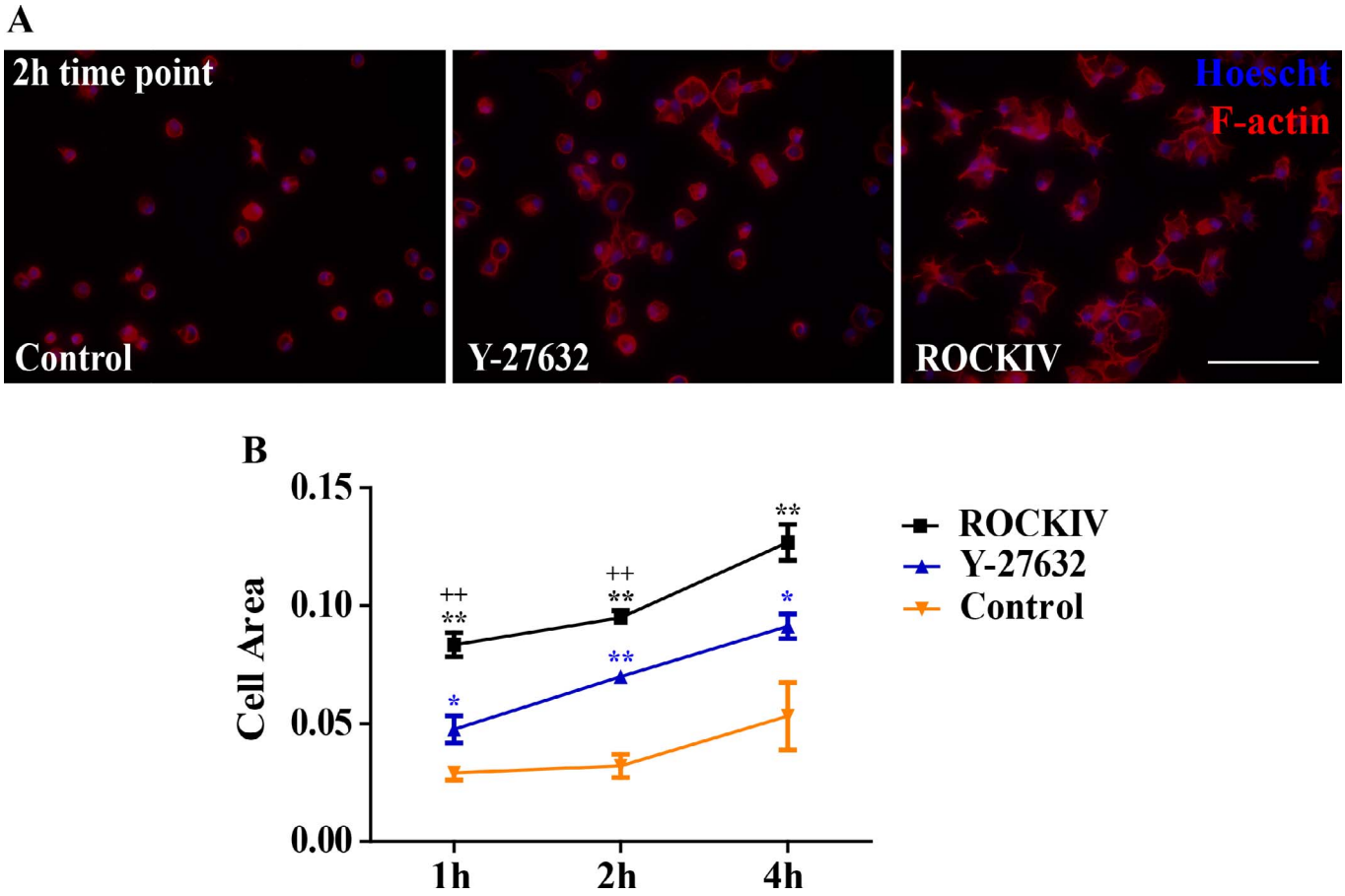

Figure 2. ROCK inhibition promotes cell spreading. (A) Fluorescent images of cells stained with phalloidin-TRITC (*red*) to visualize F-actin, and Hoescht (*blue*) to label cellular DNA were captured 2 hours after plating. *Scale bar*, 100 μm. (B) Quantification of cell area from phalloidin fluorescence. $^{*}P \leq 0.05$, $^{**}P \leq 0.01$ compared with control. $^{+}P \leq 0.05$, $^{++}P \leq 0.01$ compared with Y-27632. *Error bars* represent ± SEM ($n = 5$).

staining within the wounded area following pan-ROCK inhibition (Fig. 5B). Surprisingly, ROCK2 inhibition alone showed no changes from control in MKI67 expression patterns. As noted above, ROCK2 inhibition significantly increased the individual cell size within the scratched region compared with both control and panROCK inhibition treatments. (Fig. 5C). Importantly, there was no MKI67 expression detected 30 days post scratch in any of the treatment groups; therefore, the increase in proliferation due to panROCK inhibition did not aberrantly continue after treatment was stopped at 14 days post scratch (Supplementary Figs. 2A, 2B). Interestingly, F-actin staining 30 days post scratch showed a persistent larger cell size morphology and cell area of ROCK2 inhibited hESC-RPE cells (Supplementary Figs. 2A, 2C).

Discussion

ROCKs are thought to play an important role in stimulating EMT, and ROCK inhibition is thought to prevent the EMT, possibly via inhibition of TGF-β signaling, which often contributes to scarring following a wound.[14,31] Based on this concept, the use of synthetic ROCK inhibitors is currently being tested in several clinical trials for various diseases, including corneal epithelial wound healing.[34] Previously, we showed that ROCK inhibition increased proliferation rates of hESC-RPE cells and allowed extended passage of hESC-RPE and iPSC-RPE cells.[31] In this report, we examined the role of ROCK(s) in hESC-RPE attachment, migration, and wound healing in vitro.

It is well established that ROCK activity stabilizes actin fibers and promotes stress fiber formation

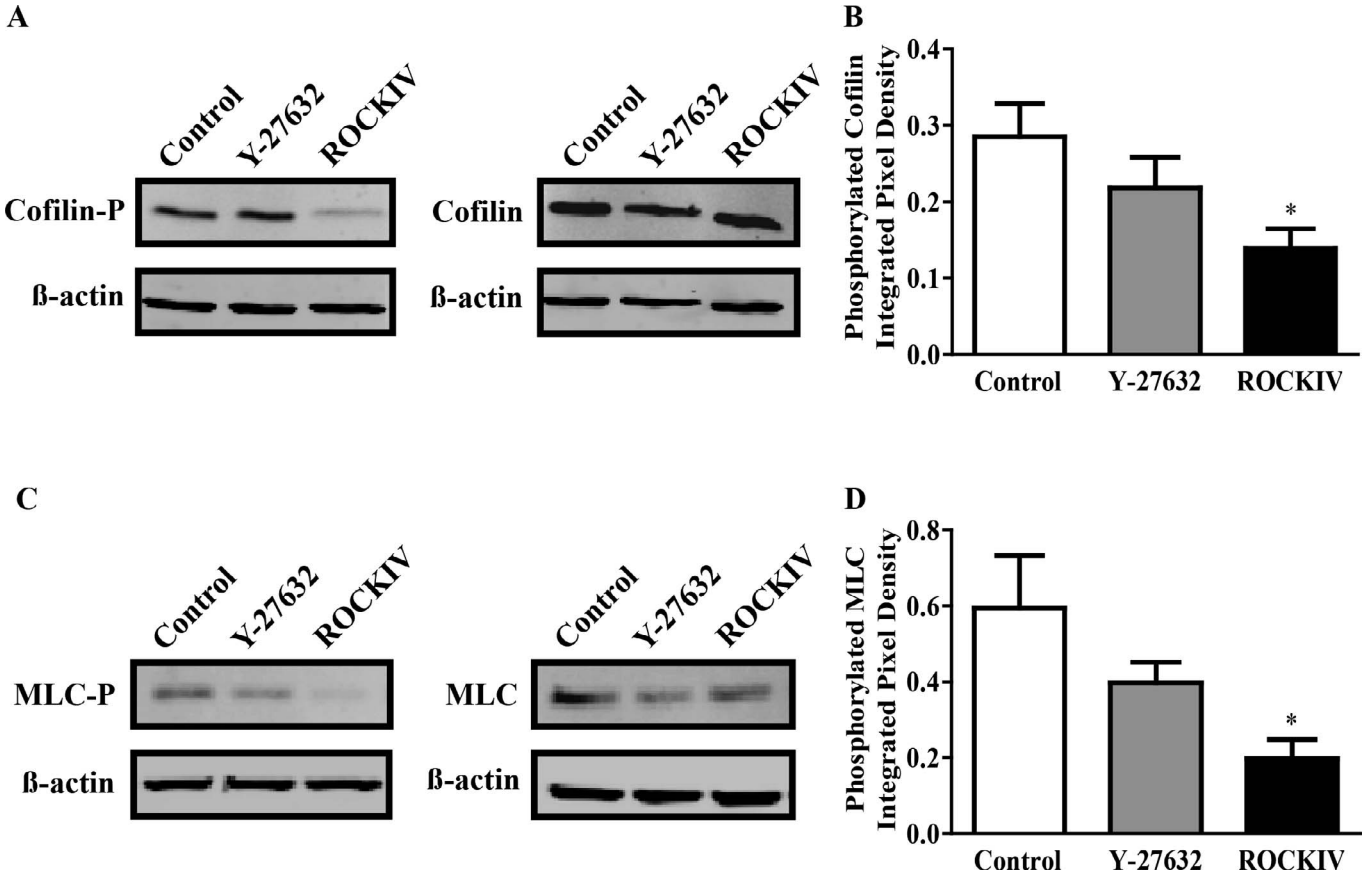

Figure 3. ROCK2 inhibition decreases cofilin and MLC phosphorylation. hESC-RPE cells were treated at the time of plating with Y-27632 or ROCKIV and protein was collected 2 hours later. (A) Total protein lysates were probed with anti–phospho-cofilin, cofilin, and β-actin antibodies. (B) Quantification of phosphorylated cofilin protein over β-actin. (C) Total protein lysates were probed with anti–phospho-MLC, MLC, and β-actin antibodies. (D) Quantification of phosphorylated MLC protein over β-actin. *$P \leq 0.05$ compared with control. *Error bars* represent ± SEM ($n \geq 4$).

through its regulation of LIMK and MLC, and therefore can increase cell attachment in certain settings.[17,35–37] LIMK is activated by ROCK1/2 and inactivates cofilin, leading to the stabilization of actin polymers.[38] Thus, ROCK inhibition would activate cofilin, leading to depolymerization of actin microfilaments.[39] Surprisingly, we found that ROCK inhibition increases cell attachment in H9 hESC-RPE cells (Fig. 1). We hypothesize that this is due to the reorganization of actin fibers that might be important in RPE adhesion. In contrast to effects reported in other cell types,[40] we found an increase in cell spreading within the first hour after plating following ROCK inhibition compared with control (Fig. 2), and that cofilin and MLC phosphorylation patterns were altered (Fig. 3). This could be an important part of the RPE adhesion process. Interestingly, there was a significantly greater effect in cell spreading with ROCK2 inhibition alone (Fig. 2), perhaps related to the fact that ROCK2 inhibition leads to a larger, mesenchymal-like cell morphology, observed within the described scratch assays (Fig. 5).

The effects of ROCK inhibition on attachment could be extremely beneficial in hESC-RPE cellular therapies involving bolus injections of cells.[10,11] It also demonstrates a new role for ROCK inhibition in attachment of H9-hESC-RPE cells. hESC-RPE cells are generally plated at a high seeding density, but through the use of ROCK inhibition, we can combine the beneficial effects of an increase in cell attachment with the known effects of increased proliferation to seed RPE cells at a lower density and save time, money, and cells. ROCK inhibition may increase attachment in other cell types and might be useful in expansion of cells as well as integration after transplant.

Aside from the implications in ocular disease, ROCK inhibition is under investigation as an antimetastatic agent to prevent migration in various cancers.[41] Many

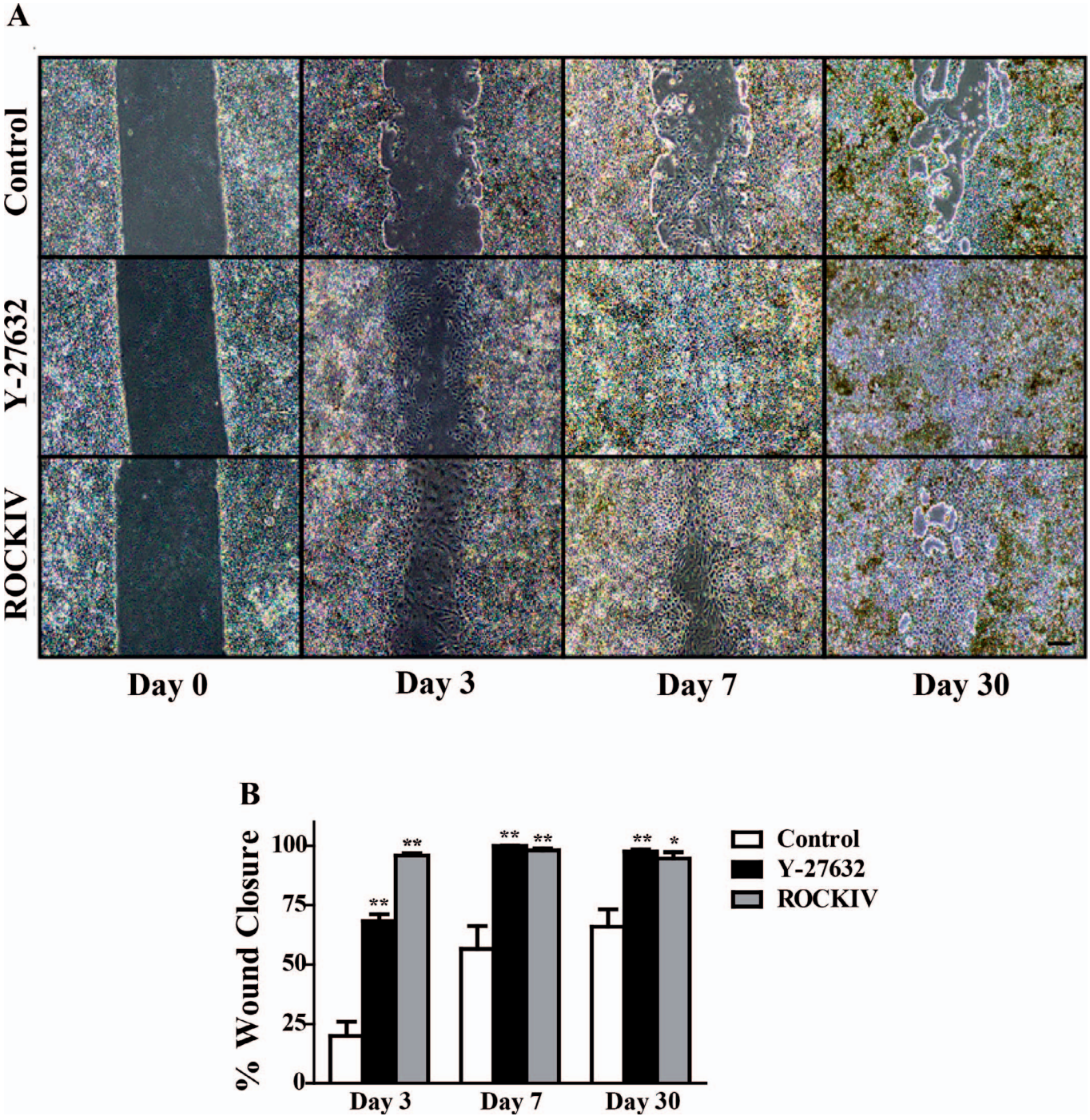

Figure 4. ROCK inhibition enhances wound closure in vitro. (A) hESC-RPE cells were scratched following 30 days in culture and treated with either Y-27632 or ROCKIV and wound closure was monitored over an additional 30 days. Control and ROCKIV-treated cells failed to completely close the wounded area. *Scale bar*, 200 μm (B) Quantification of wound closure at each time-point imaged. $^{*}P \leq 0.05$, $^{**}P < 0.01$ compared with control at that time-point. *Error bars* represent ± SEM ($n = 3$).

researchers have examined the effect of ROCK inhibition on migration, however the data presented here should open up research avenues to elucidate ROCK inhibition's role in attachment of tumor cells and EMT, characteristics of metastatic tumor cells.[42] Recent studies have shown that ROCK inhibition can promote the reattachment of breast cancer cells in circulation, which correlates with our conclusions.[43]

We also examined the roles of ROCK1/2 in an in vitro "scratch" model of RPE wound healing. We

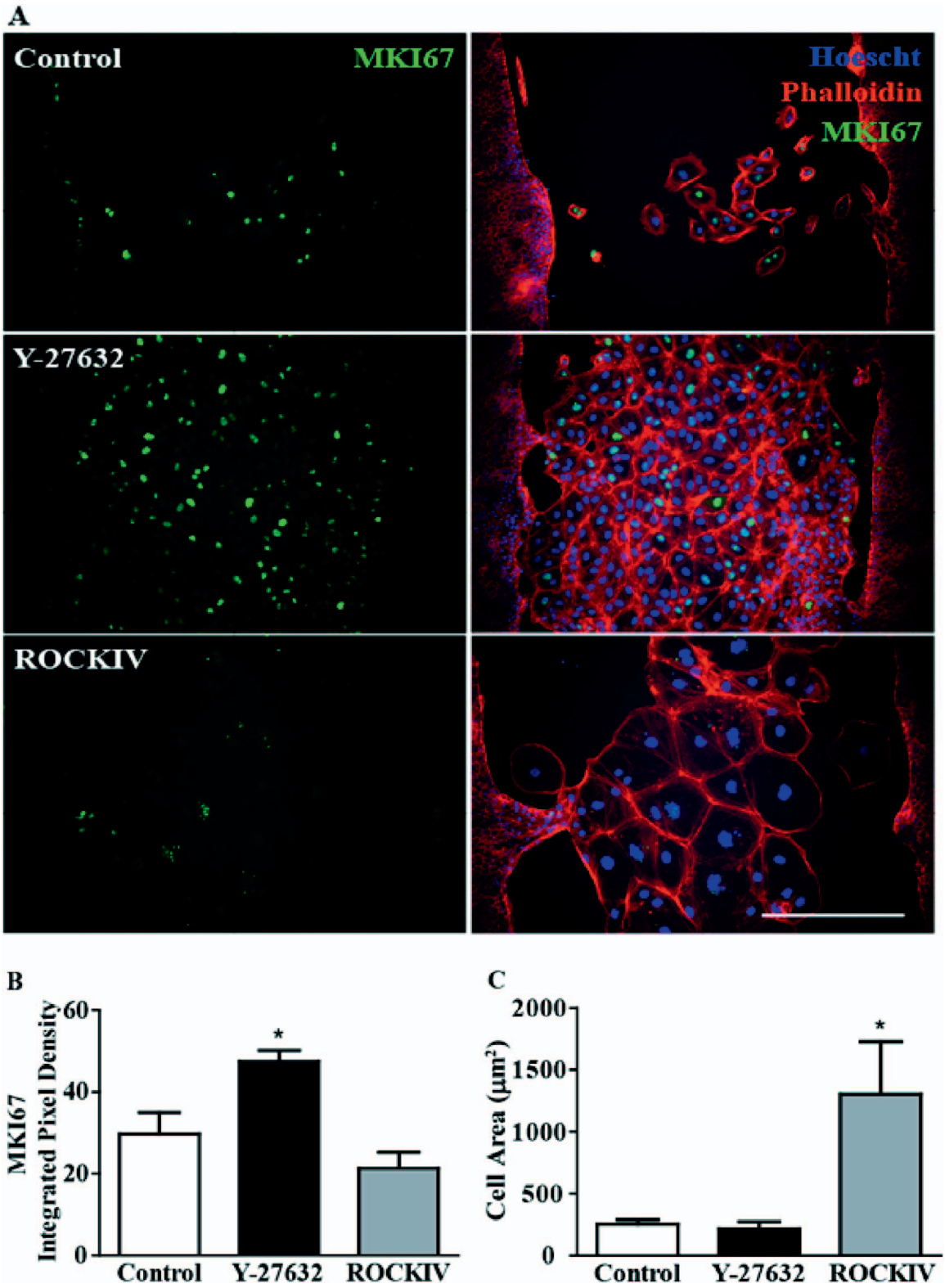

Figure 5. PanROCK inhibition promotes proliferation in wounded area. (A) Five days after scratch, cells were stained with anti-MKI67 (marker of proliferation KI67, *green*), phalloidin (F-actin, *red*), and Hoescht (DNA, *blue*). *Scale bar*, 100 μM. (B) MKI67 fluorescence in wounded area was significantly higher when cells were treated with 10 μM of Y-27632. *$P \leq 0.05$ to control (C) ROCKIV treatment increased cell size compared with control and Y-27632 treatment. *$P \leq 0.05$ to control. *Error bars* represent ± SEM ($n = 3$).

found that panROCK inhibition, but not ROCK2 inhibition alone, promoted proliferation to fill in the area devoid of cells (Figs. 4 and 5). Typical cobblestone epithelial morphology was quickly regained and the wound was closed faster than control when cells were treated with the panROCK inhibitor (Fig. 4). These data could distinguish a specific role for ROCK1 in proliferation. Importantly, this increase in proliferation was not seen outside the scratch area, and cells exited the cell cycle after the wound was closed and treatment was stopped (Fig. 5, Supplementary Fig. 2).

ROCK2 inhibites cells within the scratched region at day 5, were significantly larger and more mesenchymal-like, compared with control and panROCK inhibited treated cells (Fig. 5). PanROCK inhibition has been shown to inhibit major players in the TGF-β and EMT pathways,[31] however these morphology differences could suggest that ROCK2 inhibition alone might promote EMT. This could point toward opposing and specific roles for ROCK1 and ROCK2; ROCK2 in inhibiting EMT, while ROCK1 may promote EMT, in this system. Unfortunately, at this time there are no ROCK1 specific inhibitors; therefore, hESC-RPE knockdowns and knockouts of ROCK1 and ROCK2 need to be examined to fully test this theory. A closer examination of ROCK inhibition in wound healing could prompt a novel therapeutic for GA, a devastating progression of AMD.

RPE migration and wound response are also an important consideration in proliferative vitreal retinopathy (PVR). PVR is characterized by improper cell localization, leading to the formation of epiretinal "membranes" on the inner surface of the retina, which can contract and cause retinal detachment.[44–46] Mislocalized RPE cells are found in these membranes[45] and RPE migration and wound response are thought to be a crucial aspect of this process.[46] Thus, some caution must be exercised in any strategies that mobilize RPE cells.

It is important to note that characteristic epithelial wound healing occurs through cell sheet migration and proliferation where cells remain attached to the cell monolayer as they repopulate the wound.[47,48] This is especially evident in previous studies of MCDK cells. In our studies, the borders of the sheet are not as uniform as has been seen in Madine-Darby canine kidney epithelial cells (MDCK). H9 hESC-RPE cells migrate into the wound in an uneven fashion, and on some occasions, individual cells can be observed in the middle of the wound.

Similar migration patterns of individual cells breaking free from the monolayer have been reported in a recent study of iPS-RPE.[49] In addition, some studies of primary RPE also show many[50] or a few[51] individual cells moving in to fill the void of the wound. We note that differences in protocol must be considered as well, because previous studies have used different substrate coatings (fibronectin, laminin, or serum proteins versus matrigel), different medias, and different sizes of wound.

hESC-RPE are known to undergo EMT during passaging and proliferation, and perhaps hESC-RPE are closing the wound by a mesenchymal mechanism before reverting back to epithelial cells.[52,53] Mesenchymal cells have been shown to close wounds through a sheet-independent mechanism.[47] More work is needed to fully understand the mechanisms of wound closure in hESC-RPE cells. In addition, further research is required to examine whether primary RPE, and other hESC-RPE and iPSC-RPE lines exhibit the same trends in attachment and wound closure. Organotypic three-dimensional in vitro cultures and animal studies will also be important.

The data presented here offer initial valuable insight into the functions of specific ROCK isoforms, and inhibitors that could be used alone or in combination with cellular therapies to help restore RPE cells in various ocular diseases. Furthermore, ROCK inhibition treatment could cross over to other diseases where epithelial layers are compromised, or be used to help prevent postoperative scarring as is common in glaucoma surgeries.[34]

Acknowledgments

Supported by the California Institute for Regenerative Medicine (CIRM; DR1-01444, CL1-00521, TB1-01177, TG2-01151 and FA1-00616) , The Foundation Fighting Blindness Wynn-Gund Translational Research Acceleration Program, the Garland Initiative for Vision at UC Santa Barbara, and a grant to the University of California Santa Barbara Institute for Collaborative Biotechnologies from the US Army Research Office (W911NF-09-0001). The content within does not necessarily reflect the position or policy of the government, and endorsement should not be inferred. RHC was a fellow of the California Institute for Regenerative Medicine.

References

1. Gehrs KM, Anderson DH, Johnson LV, Hageman GS. Age-related macular degeneration–emerging pathogenetic and therapeutic concepts. *Ann Med*. 2006;38:450–471.
2. Curcio CA, Medeiros NE, Millican CL. Photoreceptor loss in age-related macular degeneration. *Invest Ophthalmol Vis Sci*. 1996;37:1236–1249.
3. Young RW. Pathophysiology of age-related macular degeneration. *Surv Ophthalmol*. 1987; 31:291–306.
4. Bowes Rickman C, Farsiu S, Toth CA, Klingeborn M. Dry age-related macular degeneration: mechanisms, therapeutic targets, and imaging. *Invest Ophthalmol Vis Sci*. 2013;54:ORSF68–ORSF80.
5. Age-Related Eye Disease Study Research Group. A randomized, placebo-controlled, clinical trial of high-dose supplementation with vitamins C and E, beta carotene, and zinc for age-related macular degeneration and vision loss: AREDS report no. 8. *Arch Ophthalmol*. 2001;119:1417–1436.
6. Bird AC. Therapeutic targets in age-related macular disease. *J Clin Invest*. 2010;120:3033–3041.
7. Ferris FL III, Wilkinson CP, Bird A, et al. Clinical classification of age-related macular degeneration. *Ophthalmology*. 2013;120:844–851.
8. Ramsden CM, Powner MB, Carr AJ, Smart MJ, da Cruz J, Coffey PJ. Stem cells in retinal regeneration: past, present and future. *Development*. 2013;140:2576–2585.
9. Croze RH, Clegg DO. Differentiation of pluripotent stem cells into retinal pigmented epithelium. In: Zarbin MA, Casaroli-Marano RP, eds. *Cell-Based Therapy for Retinal Degenerative Disease. Developmental Ophthalmology*. Basel, Switzerland: Karger; 2014; 81–96.
10. Schwartz SD, Hubschman JP, Heilwell G, et al. Embryonic stem cell trials for macular degeneration: a preliminary report. *Lancet*. 2012;379: 713–720.
11. Schwartz SD, Regillo CD, Lam BL, et al. Human embryonic stem cell-derived retinal pigment epithelium in patients with age-related macular degeneration and Stargardt's macular dystrophy: follow-up of two open-label phase 1/2 studies. *Lancet*. 2015;385:509–516.
12. Nazari H, Zhang L, Zhu D, et al. Stem cell based therapies for age-related macular degeneration: the promises and the challenges. *Prog Retin Eye Res*. 2015;48:1–39.
13. Weber CE, Li NY, Wai PY, Kuo PC. Epithelial-mesenchymal transition, TGF-beta, and osteopontin in wound healing and tissue remodeling after injury. *J Burn Care Res*. 2012;33:311–38.
14. Wynn TA. Common and unique mechanisms regulate fibrosis in various fibroproliferative diseases. *J Clin Invest*. 2007;117:524–529.
15. Leoni G, Neumann PA, Sumagin R, Denning TI, Nusrat A. Wound repair: role of immune-epithelial interactions. *Mucosal Immunol*. 2015;8: 959–968.
16. Abreu-Blanco MT, Watts JJ, Verboon JM, Parkhurst SM. Cytoskeleton responses in wound repair. *Cell Mol Life Sci*. 2012;69:2469–2483.
17. Vardouli L, Moustakas A, Stournaras C. LIM-kinase 2 and cofilin phosphorylation mediate actin cytoskeleton reorganization induced by transforming growth factor-beta. *J Biol Chem*. 2005;280:11448–11457.
18. Jarvinen PM, Laiho M. LIM-domain proteins in transforming growth factor beta-induced epithelial-to-mesenchymal transition and myofibroblast differentiation. *Cell Signal*. 2012;24:819–825.
19. Zandi S, Nakao S, Chun KH, et al. ROCK-isoform-specific polarization of macrophages associated with age-related macular degeneration. *Cell Rep*. 2015;10:1173–1186.
20. Surma M, Handy C, Chang J, Kapur R, Wei L, Shi J. ROCK1 deficiency enhances protective effects of antioxidants against apoptosis and cell detachment. *PLoS One*. 2014;9:e90758.
21. Lee SH, Huang H, Choi K, et al. ROCK1 isoform-specific deletion reveals a role for diet-induced insulin resistance. *Am J Physiol Endocrinol Metab*. 2014;306:E332–E343.
22. Mertsch S, Thanos S. Opposing signaling of ROCK1 and ROCK2 determines the switching of substrate specificity and the mode of migration of glioblastoma cells. *Mol Neurobiol*. 2014;49:900–915.
23. Hahmann C, Schroeter T. Rho-kinase inhibitors as therapeutics: from pan inhibition to isoform selectivity. *Cell Mol Life Sci*. 2010;67:171–177.
24. Pan P, Shen M, Yu H, Li Y, Li D, Hou T. Advances in the development of Rho-associated protein kinase (ROCK) inhibitors. *Drug Discov Today*. 2013;18:1323–1333.
25. Shaw D, Hollingworth G, Soldermann N, et al. Novel ROCK inhibitors for the treatment of pulmonary arterial hypertension. *Bioorg Med Chem Lett*. 2014;24:4812–4817.
26. Rath N, Olson MF. Rho-associated kinases in tumorigenesis: re-considering ROCK inhibition for cancer therapy. *EMBO Rep*. 2012;13:900–908.

27. Harrison BA, Almstead ZY, Burgoon H, et al. Discovery and development of LX7101, a dual LIM-kinase and ROCK inhibitor for the treatment of glaucoma. *ACS Med Chem Lett*. 2015;6:84–88.
28. Alokam R, Singhal S, Srivathsav GS, et al. Design of dual inhibitors of ROCK-I and NOX2 as potential leads for the treatment of neuroinflammation associated with various neurological diseases including autism spectrum disorder. *Mol Biosyst*. 2015;11:607–617.
29. Lu Q, Longo FM, Zhou H, Massa SM, Chen YH. Signaling through Rho GTPase pathway as viable drug target. *Curr Med Chem*. 2009;16:1355–1365.
30. Zhang T, Wei Y, Jiang X, Li J, Qiu S, Zhang S. Protection of photoreceptors by intravitreal injection of the Y27632 Rhoassociated protein kinase inhibitor in Royal College of Surgeons rats. *Mol Med Rep*. 2015;12:3655–3661.
31. Croze RH, Buchholz DE, Radeke MJ, et al. ROCK inhibition extends passage of pluripotent stem cell-derived retinal pigmented epithelium. *Stem Cells Transl Med*. 2014;3:1066–1078.
32. Schindelin J, Arganda-Carrereas I, Frise E, et al. Fiji: an open-source platform for biological-image analysis. *Nature Methods*. 2012;9:676–682.
33. Kosako H, Yoshida T, Matsumura F, Ishizaki T, Narumiya S, Inagaki M. Rho-kinase/ROCK is involved in cytokinesis through the phosphorylation of myosin light chain and not ezrin/radixin/moesin proteins at the cleavage furrow. *Oncogene*. 2000;19:6059–6064.
34. Wang SK, Chang RT. An emerging treatment option for glaucoma: Rho kinase inhibitors. *Clin Ophthalmol*. 2014;8:883–890.
35. Yang S, Kim HM. The RhoA-ROCK-PTEN pathway as a molecular switch for anchorage dependent cell behavior. *Biomaterials*. 2012;33:2902–2915.
36. Peh GS, Adnan K, George BL, et al. The effects of Rho-associated kinase inhibitor Y-27632 on primary human corneal endothelial cells propagated using a dual media approach. *Sci Rep*. 2015;5:9167.
37. Rentala S, Chintala R, Guda M, Chintala M, Komarraju AL, Mangomoori LN. Atorvastatin inhibited Rho-associated kinase 1 (ROCK1) and focal adhesion kinase (FAK) mediated adhesion and differentiation of CD133+CD44+ prostate cancer stem cells. *Biochem Biophys Res Commun*. 2013;441:586–592.
38. Pritchard CA, Hayes L, Wojnowski L, Zimmer A, Marais RM, Norman JC. B-Raf acts via the ROCKII/LIMK/cofilin pathway to maintain actin stress fibers in fibroblasts. *Mol Cell Biol*. 2004;24:5937–5952.
39. Kim JI, Kwon J, Baek I, Park HS, Na S. Cofilin reduces the mechanical properties of actin filaments: approach with coarse-grained methods. *Phys Chem Chem Phys*. 2015;17:8148–8158.
40. Ye N, Verma D, Meng F, Davidson MW, Suffoletto K, Hua SZ. Direct observation of alpha-actinin tension and recruitment at focal adhesions during contact growth. *Exp Cell Res*. 2014;327:57–67.
41. Kale VP, Hengst JA, Desai DH, Amin SG, Yun JK. The regulatory roles of ROCK and MRCK kinases in the plasticity of cancer cell migration. *Cancer Lett*. 2015;361:185–196.
42. Tsubaki M, Komai M, Fujimoto S, et al. Activation of NF-kappaB by the RANKL/RANK system up-regulates snail and twist expressions and induces epithelial-to-mesenchymal transition in mammary tumor cell lines. *J Exp Clin Cancer Res*. 2013;32:62.
43. Bhandary L, Whipple RA, Vitolo MI, et al. ROCK inhibition promotes microtentacles that enhance reattachment of breast cancer cells. *Oncotarget*. 2015;6:6251–6266.
44. Ryan SJ. The pathophysiology of proliferative vitreoretinopathy in its management. *Am J Ophthalmol*. 1985;100:188–193.
45. Pastor JC, Rojas J, Pastor-Idoate S, Di Lauro S, Gonzalez-Buendia L, Delgado-Tirado S. Proliferative vitreoretinopathy: a new concept of disease pathogenesis and practical consequences. *Prog Retin Eye Res*. 2016;51:125–155.
46. Chen Z, Shao Y, Li X. The roles of signaling pathways in epithelial-to-mesenchymal transition of PVR. *Mol Vis*. 2015;21:706–710.
47. Matsubayashi Y, Ebisuya M, Honjoh S, Nishida E. ERK activation propagates in epithelial cell sheets and regulates their migration during wound healing. *Curr Biol*. 2004;14:731–735.
48. Rosen P, Misfeldt DS. Cell density determines epithelial migration in culture. *Proc Natl Acad Sci U S A*. 1980;77:4760–4763.
49. Por ED, Greene WA, Burke TA, Wang HC. Trichostatin A inhibits retinal pigmented epithelium activation in an in vitro model of proliferative vitreoretinopathy. *J Ocul Pharmacol Ther*. 2016;32:415–424.
50. Klettner A, Tahmaz N, Dithmer M, Richert E, Roider J. Effects of aflibercept on primary RPE cells: toxicity, wound healing, uptake and phagocytosis. *Br J Ophthalmol*. 2014;98:1448–1452.

51. Calton MA, Vollrath D. The mTOR kinase inhibitor INK128 blunts migration of cultured retinal pigment epithelial cells. *Adv Exp Med Biol*. 2016;854:709–715.
52. Grisanti S, Guidry C. Transdifferentiation of retinal pigment epithelial cells from epithelial to mesenchymal phenotype. *Invest Ophthalmol Vis Sci*. 1995;36:391–405.
53. Burke JM. Epithelial phenotype and the RPE: is the answer blowing in the Wnt? *Prog Retin Eye Res*. 2008;27:579–595.